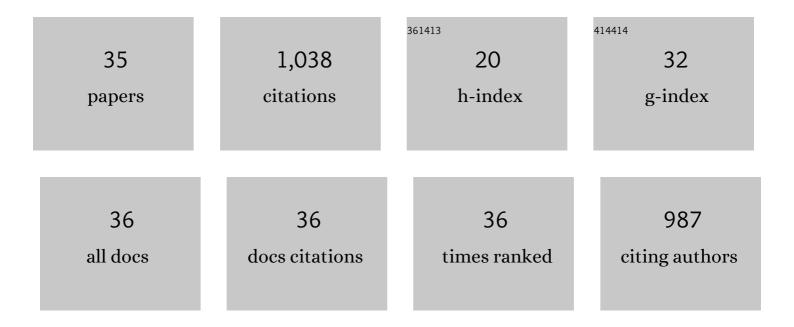
Ridong Wang

List of Publications by Year in descending order

Source: https://exaly.com/author-pdf/5004741/publications.pdf

Version: 2024-02-01



RIDONG WANG

#	Article	lF	CITATIONS
1	Inkjet-printed microelectrodes on PDMS as biosensors for functionalized microfluidic systems. Lab on A Chip, 2015, 15, 690-695.	6.0	113
2	A thermal activated and differential self-calibrated flexible epidermal biomicrofluidic device for wearable accurate blood glucose monitoring. Science Advances, 2021, 7, .	10.3	91
3	A flexible electrochemical glucose sensor with composite nanostructured surface of the working electrode. Sensors and Actuators B: Chemical, 2016, 230, 801-809.	7.8	71
4	Measurement of the thermal conductivities of suspended MoS ₂ and MoSe ₂ by nanosecond ET-Raman without temperature calibration and laser absorption evaluation. Nanoscale, 2018, 10, 23087-23102.	5.6	51
5	Frequency-domain energy transport state-resolved Raman for measuring the thermal conductivity of suspended nm-thick MoSe2. International Journal of Heat and Mass Transfer, 2019, 133, 1074-1085.	4.8	48
6	A continuous glucose monitoring device by graphene modified electrochemical sensor in microfluidic system. Biomicrofluidics, 2016, 10, 011910.	2.4	47
7	The hot carrier diffusion coefficient of sub-10 nm virgin MoS ₂ : uncovered by non-contact optical probing. Nanoscale, 2017, 9, 6808-6820.	5.6	46
8	Photothermal phenomenon: Extended ideas for thermophysical properties characterization. Journal of Applied Physics, 2022, 131, .	2.5	46
9	Nonmonotonic thickness-dependence of in-plane thermal conductivity of few-layered MoS ₂ : 2.4 to 37.8 nm. Physical Chemistry Chemical Physics, 2018, 20, 25752-25761.	2.8	45
10	Graphene Aerogel Based Bolometer for Ultrasensitive Sensing from Ultraviolet to Far-Infrared. ACS Nano, 2019, 13, 5385-5396.	14.6	42
11	Energy Transport State Resolved Raman for Probing Interface Energy Transport and Hot Carrier Diffusion in Few-Layered MoS ₂ . ACS Photonics, 2017, 4, 3115-3129.	6.6	41
12	Anisotropic thermal conductivities and structure in lignin-based microscale carbon fibers. Carbon, 2019, 147, 58-69.	10.3	37
13	Hot carrier transfer and phonon transport in suspended nm WS2 films. Acta Materialia, 2019, 175, 222-237.	7.9	34
14	Distinguishing Optical and Acoustic Phonon Temperatures and Their Energy Coupling Factor under Photon Excitation in nm 2D Materials. Advanced Science, 2020, 7, 2000097.	11.2	34
15	DNA-Based Biosensors for the Biochemical Analysis: A Review. Biosensors, 2022, 12, 183.	4.7	32
16	Thermal transport and energy dissipation in two-dimensional Bi2O2Se. Applied Physics Letters, 2019, 115, .	3.3	28
17	Thermal conductivity of SiC microwires: Effect of temperature and structural domain size uncovered by 0 K limit phonon scattering. Ceramics International, 2018, 44, 11218-11224.	4.8	25
18	Thermal behavior of materials in laser-assisted extreme manufacturing: Raman-based novel characterization. International Journal of Extreme Manufacturing, 2020, 2, 032004.	12.7	25

RIDONG WANG

#	Article	IF	CITATIONS
19	Very fast hot carrier diffusion in unconstrained MoS ₂ on a glass substrate: discovered by picosecond ET-Raman. RSC Advances, 2018, 8, 12767-12778.	3.6	24
20	Characterization of anisotropic thermal conductivity of suspended nm-thick black phosphorus with frequency-resolved Raman spectroscopy. Journal of Applied Physics, 2018, 123, .	2.5	23
21	Interfacial Thermal Conductance between Monolayer WSe ₂ and SiO ₂ under Consideration of Radiative Electron–Hole Recombination. ACS Applied Materials & Interfaces, 2020, 12, 51069-51081.	8.0	18
22	Interfacial Thermal Conductance between Mechanically Exfoliated Black Phosphorus and SiO <i>_x</i> : Effect of Thickness and Temperature. Advanced Materials Interfaces, 2017, 4, 1700233.	3.7	16
23	Polarized Raman of Nanoscale Two-Dimensional Materials: Combined Optical and Structural Effects. Journal of Physical Chemistry C, 2019, 123, 23236-23245.	3.1	16
24	In situ investigation of annealing effect on thermophysical properties of single carbon nanocoil. International Journal of Heat and Mass Transfer, 2020, 151, 119416.	4.8	15
25	Identifying the Crystalline Orientation of Black Phosphorus by Using Optothermal Raman Spectroscopy. ChemPhysChem, 2017, 18, 2828-2834.	2.1	12
26	Direct Characterization of Thermal Nonequilibrium between Optical and Acoustic Phonons in Graphene Paper under Photon Excitation. Advanced Science, 2021, 8, 2004712.	11.2	12
27	Energy and Charge Transport in 2D Atomic Layer Materials: Raman-Based Characterization. Nanomaterials, 2020, 10, 1807.	4.1	8
28	The in-plane structure domain size of nm-thick MoSe ₂ uncovered by low-momentum phonon scattering. Nanoscale, 2021, 13, 7723-7734.	5.6	7
29	Methods for Measuring Thermal Conductivity of Two-Dimensional Materials: A Review. Nanomaterials, 2022, 12, 589.	4.1	7
30	Thermal conductance between water and nm-thick WS ₂ : extremely localized probing using nanosecond energy transport state-resolved Raman. Nanoscale Advances, 2020, 2, 5821-5832.	4.6	6
31	A Fiber-Based SPR Aptasensor for the In Vitro Detection of Inflammation Biomarkers. Micromachines, 2022, 13, 1036.	2.9	5
32	A Method for Measuring the Volume of Transdermally Extracted Interstitial Fluid by a Three-Electrode Skin Resistance Sensor. Sensors, 2014, 14, 7084-7095.	3.8	4
33	Asymmetry of Raman scattering by structure variation in space. Optics Express, 2017, 25, 18378.	3.4	4
34	A high-accuracy measurement method of glucose concentration in interstitial fluid based on microdialysis. Measurement Science and Technology, 2017, 28, 115701.	2.6	3
35	Pressure self-compensation for humidity sensing using graphene-oxide-modified dual-frequency CMUT. Sensors and Actuators B: Chemical, 2020, 314, 128074.	7.8	2